GEOLOGICAL, GEOCHEMICAL AND SPECTROMETRIC STUDIES ON THE TRACHYTE DYKES OF WADI EL HORA AREA, SOUTH EASTERN DESERT, EGYPT

IBRAHIM B. ABD EL KADER
Nuclear Materials Authority. P.O. 530 El Maadi, Cairo, Egypt
E-mail: ibrahim_badie_geo@yahoo.com

ABSTRACT

Wadi El Hora Phanerozoic alkaline trachyte dykes are located at the southern Eastern Desert of Egypt. These trachyte dykes are located between two strike-slip faults taking the N-S and NW-SE trend. The alkaline trachyte dykes consist essentially of feldspars (albite, oligoclase and sanidine), quartz, and alkali pyroxene (aegirine and aegirine-augite) with zircon, fluorite and opaques as accessory minerals, and finally kaoline and sericite as secondary minerals.

The trachyte dykes are rich in high field strength elements Nb, Zr, and Y, they also exhibit typical extensional tectonic alkaline magmatisms and evolved in within plated environment. Rare earth elements (REE) patterns exhibit negative Eu anomalies and are largely uniform and heavily fractionated. These trachyte dykes could be considered as a good target for columbite and zircon exploration. According to a detailed spectrometric analysis, the radioelement concentrations are controlled by post magmatic redistribution since the eU/eTh ratio changed directly with eU concentrations and scattered with eTh. The radiometric measurements of trachyte dykes in the study area show a very wide variation in eU (0.6 – 197.1 ppm with an average 43.73) and eTh (2.4 – 626.3 ppm with an average 109.35) contents. The mineralogical study confirms the presence of kasolite, columbite, zircon, fluorite, molybdenite, monazite, pyrite and ilmenite minerals.

Keywords: Trachyte dykes, Geochemical, Spectrometric Studies, Columbite.

INTRODUCTION

Wadi El Hora is found at about 8 km southwest of Darhib talc mine and about 40 km southeast of El Sheikh Shadli at the southern Eastern Desert of Egypt at latitudes $23^o51^\backslash48^{\backslash\backslash}$ and $24^o00^\backslash51^{\backslash\backslash}$ and between longitudes $34^o50^\backslash11^{\backslash\backslash}$ and $34^o58^\backslash46^{\backslash\backslash}$ with area about 225 km^2 (Fig. 1). This study deals with geological, geochemical and spectrometric studies of the alkaline trachyte dykes in the area which are located between N-S and NW-SE two strike-slip faults. These alkaline trachyte dykes consist essentially of feldspars (albite, oligoclase and sanidine), quartz, and alkali pyroxene (aegirine and aegirine-augite) with zircon, fluorite and opaques as accessory minerals, and

finally kaoline and sericite as secondary minerals.

At the end of the Pan-African event (650-550 Ma), the calc-alkaline arc-related magmatism was replaced by calc-alkaline to alkaline post-orogenic magmatism (Abdel-Rahman 1995). The Arabian-Nubian Shield crust is thought to have formed during the Pan-African event (950–550 Ma) as a result of the rapid subduction of many island arcs, according to Kröner, 1985 and Stoeser, 1986. This arc system stabilized as a result of its accumulation and subsequent sweeping together.
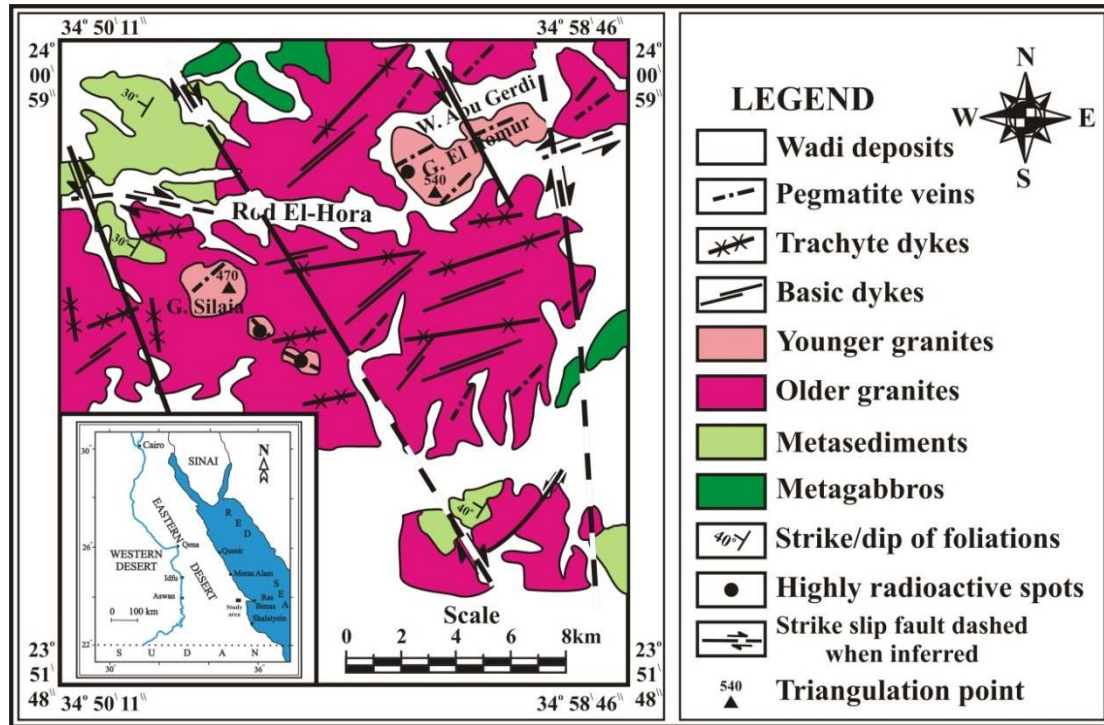
Fig. 1: Geologic map of Wadi El Hora area, south Eastern Desert, Egypt (after Saleh, 2012).

According to Harris (1982), the Arabian–Nubian Shield was heavily invaded by plutonic to volcanic basic to acidic, and alkaline to peralkaline rocks. These igneous rocks are the surface manifestations of within-plate or A-type magmatism that occurred during the anorogenic tectonic-magmatic phase of the Arabian-Nubian Shield.

El-Manharawy (1972), Hashad and Mahfouz (1976), Hashad et al. (1981), Kamel et al. (1985), Akaad (1996), Ibrahim et al. (2002), Amer et al. (2002), Heikal (2003), and Saleh et al. (2021) are practically researchers who have previously studied the alkaline granitic complexes in the area. For the Paleozoic volcanics in Egypt, Meneisy (1990) proposed three primary volcanic episodes, encompassing the Late Carboniferous, Permian and Permo-Traissic periods. These volcanic rocks include a wide range of rock types, including latites, bostonites, andesites, basalts and rhyolites (Aly and Moustafa, 1984).

Long-lasting volcanic activity in Egypt demonstrates a shift in tectonic setting from ocean floor and subduction-related volcanics in the Precambrian to intraplate volcanicity in the Phanerozoic. The effect of these complex tectonic regimes may be seen in changes in the composition of developed rocks throughout time. Numerous geochronological analyses of these Phanerozoic volcanics have shown three stages of activity in Egypt (El-Shazly,

1977, Hashad et al., 1978, Ressetar et al., 1981, Stairs et al., 1991). These are, Paleozoic (233-395 Ma), Mesozoic (74-191 Ma) and Tertiary (15-48 Ma). The tectono-magmatic events that had affected the Eastern Desert of Egypt during the Mesozoic Era are the causes of these dykes.

Generally, during the last two decades, a considerable investigation for the origin of continental intraplate alkaline rock series ranging from mildly alkaline or transitional basalts to peralkaline trachyte or rhyolites as it is a complex process (Saleh et al., 2004, 2007, 2015, 2021, El Tohamy, 2011, Hamdy et al., 2017, Ali et al., 2022, Abdalla et al., 2023). Numerous evolutionary and petrogenetic models have been suggested as: a) a crystal fractionation of mantle–derived magma (Price et al., 1985), b) a trachyte melts due to interaction of mantle-derived magmas with crustal materials (Davidson and Wilson, 1989), c) a process of magma mixing (Gourgaud and Maury, 1984) and d) injection of volatile-rich basic magma of mantle origin that induced partial melting of the lower crust (Bailey, 1980). The alkaline volcanic rocks emerge to host uranium are more than sub-alkaline and calc-alkaline assortment (Leroy and Aniel, 1991).

GEOLOGIC SETTING AND PETROGRAPHY

Gabal El Homur and Gabal El Silaia in Wadi El Hora area; are two distinct neighbors of younger granites that can be described as the main topographical landmarks in the study area. Hunting, (1967), Soliman, (1975), El Amin and Bassiony (1987) and Ghazaly (1996) had been described them in the previous literatures as two feldspars tectonic younger granites of intrusive character. There are many low relief older granites surrounding the two granitic intrusions, and exposed as scattered masses in wide sand plain. G.

El Silaia and Banat El Silaia (the associated small stocks) are described as pink coarse granites and are perhaps confined to one fault zone (El Ramly et al., 1971). Hashad and El Reedy (1979) determined the age of G. El Silaia as 221 ±12 m.y. age using an Rb/Sr isotope, confirming that it belongs to the alkaline suite of Egypt, that related to Mesozoic Era and agree with El Ramly et al., (1971).

Detailed field studies revealed that the area comprises the main lithologic rock types beginning from the oldest to the youngest as follow: metagabbros, metasediments, older granites, younger granites (monzogranites), and trachyte dykes. The metagabbros exhibit a wide variation of colors, varying from dark grey, dark green to lighter green due to variations in the relative proportions of felsic and mafic phases. These metagabbro show moderate relief and the most prominent topographic features are represented by the ridges that mainly oriented in NW - SE due to the NW - SE structure trend affecting this rock unit. A number of pegmatite veins (about 10 m length) are present as either parallel to or cross the layering planes intruding these rocks.

Biotite and hornblende schists are examples of the metasediments. They form relatively low relief terrain (about 250 m.a.s.l.), which extend NNW-SSE near the most upper stream of Wadi El Hora. These rocks are fine grained and greyish white in color, showing platy and/or fibrous crystals and extend beyond the mapped area in the SSE direction. The metasediments' foliations run parallel to the NNW-SSE right lateral strike slip fault (Fig. 2). Some acidic and basic dykes running ENE-WSW and cutting the metasediments.

Fig. 2: View showing the foliation in metasediments is parallel to the strike of the NNW - SSE right lateral strike slip fault.

The older granites are generally low to moderate in topography (Fig. 3). They have a whitish grey tint and are medium to coarse-grained in hand specimens. They are sheared, especially around the faults affecting the extreme of the studied area. This shearing could be attributed to the intensive faulting affecting these masses. Also they are fractured, lineated with lineation and dipping steeply towards the east direction. Mullion structures and ribbing are very well marked on the foliation surfaces. Numerous quartz and pegmatite veins, as well as basic dykes, cut and cross these rocks. These dykes are striking N45^o E and dipping 50° toward NE. Several Schist xenoliths are found within these rocks.

Fig. 3: View showing the older granites are characterized by relatively low to medium topography.

The younger granites (monzogranites) (Fig. 4) are exposed at the southwestern and northeastern sides of the mapped area (Fig. 1). They are represented by G. El Homur and G. El Silaia. G. El Silaia is moderate relief, covering about 20 km^2, and form

elongated mass in NNW-SSE direction. G. El Homur occupies large area at NE of the downstream of W. El Hora. They are intruded the older granites in sharp intrusive contact. They are pinkish white in color and massive. NNW-SSE dextral strike slip faults dislocate G. El Homur monzogranites with 3.3km. displacement. Numerous swarms of dykes, quartz and pegmatite veins, striking N 50° W-S 50° E with a dip 35° toward NE cut through G. El Homur. Many alterations are well distinct around the boundaries of the monzogranites, represented by hematitization and kaolinitization. Radioactive anomaly is recorded of these alterations. The basic dykes represent the majority of the dykes in the area, exceed 0.25-0.50 m in thickness, and striking NE-SW. Pegmatites are found as veins, dykes, pockets and irregular bodies of various dimensions and thicknesses, they are ranging from few centimeters to few meters in width and hundreds of meters in length.

Fig. 4: View showing younger granites (monzogranites) are characterized by low to medium topography.

The trachyte dykes are the youngest rock type in the studied area. The Gabal El Homur and Gabal El Silaia comprise two significant masses (approximately 1.5 km^2) with few sheets and dykes. The trachyte dykes dip outward in all directions and always makes sharp contact with the metagabbros. Along the northerly directions of Gabal El Homur and Gabal El Silaia, other minor trachyte dykes are dispersed. The trachyte dykes intrude the two monzogranites, having a NE-SW

and ENE-WSE direction and are nearly vertical.

The trachyte dykes in Wadi El Hora area are shown in Figure (5), as fine-grained rocks with a range of brown, greenish, or pinkish-gray colours. Petrographically, they are composed of quartz, alkali feldspars (sanidine) and alkali pyroxene (aegirine and aegirine augite) set in a fine grained groundmass which shows the characteristic trachytic texture (Fig. 6). Secondary minerals are represented by sericite, chlorite, muscovite and epidote, while zircon, fluorite and opaques are the accessories.

Fig. 5: Views showing trachyte dykes, Wadi El Hora area, South Eastern Desert, Egypt.
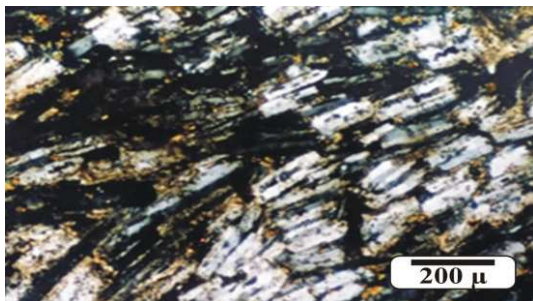
Fig. 6: Photomicrograph showing trachytic texture, Wadi El Hora area, South Eastern Desert, Egypt.

Quartz is found as small anhedral to subhedral fine grains in the groundmass. It contains inclusions of zircon. Sanidine is subhedral and found as the main feldspar. Aegirine-augite occurs as black to greenish-black subhedral crystals associated with feldspars (Fig. 7). Aegirine is found as pale brown or brown subhedral crystal (Fig. 8). Zircon occurs as fine prismatic crystals in the groundmass and as inclusions in quartz. It occurs as minute crystals showing abnormal interference color. Pyrite is an euhedral crystal associated with K-feldspars as an abundant sulfides. Opaques are found as aggregates of anhedral crystals associated with feldspar. Fluorite is also present as minute cubic crystals, recognized by its isotropic character.
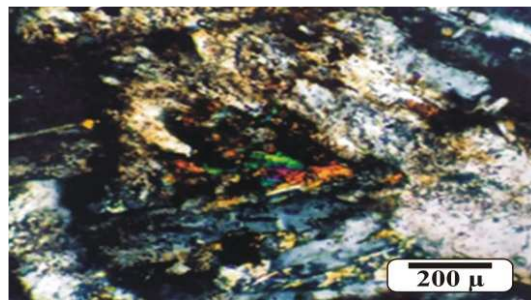
Fig. 7: Photomicrograph showing subhedral prismatic crystals of aegirine-augite, Wadi El Hora area, South Eastern Desert, Egypt.
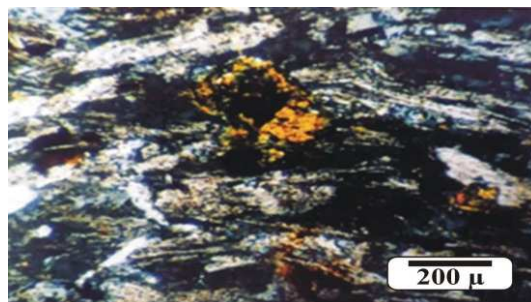
Fig. 8: Photomicrograph showing subhedral crystals of aegirine, Wadi El Hora area, South Eastern Desert, Egypt.

ANALYTICAL METHODS

This study involves the following: -

Sampling of 16 rock samples from the studied trachyte dykes, and using the portable gamma-ray spectrometer (RS-230) to survey the area radiometrically. Preparation of

thin sections for detailed petrographic studies. Sixteen representative samples were analyzed for major oxides and trace elements as well as rare earth elements for eight samples. Crushing, grinding, grain size analysis and heavy liquid separation were done to determine the heavy minerals content. At the labs of the Nuclear Materials Authority (NMA), Egypt, mineralogical studies using binocular microscope with verification and examination of some selected mineral grains using the Environmental Scanning Electron Microscope (ESEM) technology [Model XL 30 with Energy Dispersive X-ray (EDX) from Phillips]. Total gamma radiations in the field were measured using the portable RS-230 gamma ray spectrometer device.

MINERALOGY

The studied minerals were examined by the Environmental Scanning Electron Microscope (ESEM) supported by Energy Dispersive Spectrometer (EDS) unit at the Nuclear Materials Authority of Egypt. The mineralogical study of the trachyte samples revealed the presence of kasolite, monazite, fluorite, columbite, molybdenite, zircon, pyrite and ilmenite minerals (Figs. 9:16).

3.a. Kasolite $Pb(UO_2)SiO_4.H_2O$

In general, it is ocher-yellow to brownish yellow amber-brown, rarely lemon-yellow to green or reddish orange. It is occurred due to the oxidation of uraninite mineral. It is confirmed by ESEM and contains 44.55% U, 32.65% Pb, 9.12% Si and 4.14% K (Fig. 9).
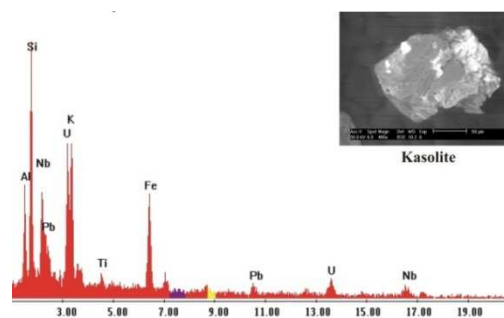
Fig. 9: ESEM image and EDX analysis data of a) kasolite, Wadi El Hora area, South Eastern Desert, Egypt.

3.b. Monazite $(Nd, La, Ce)PO_4$

Monazite is a common light REEs bearing mineral and it is also an ultra-stable mineral during weathering. It is bright rose-red in color. It sometimes makes a continuous series with huttonite $(ThSiO_{4)}$ due to the coupled substitution between $Th^{4+} \ Si^{4+} \rightleftharpoons Ce^{3+} \ P^{5+}$ in the two minerals as an isostructural (Deer et al, 1992). It is confirmed by ESEM and contains 28.66% P, 17.57% Ce, 13.75% La, 4.18% Ce and 1.24% Sm (Fig. 10).
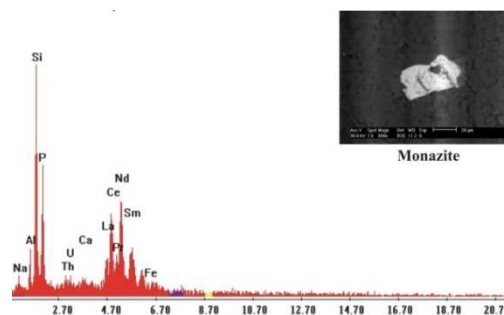
Fig. 10: ESEM image and EDX analysis data of monazite, Wadi El Hora area, South Eastern Desert, Egypt.

3.c. Fluorite CaF_2

Fluorite is found as anhedral crystals that vary greatly in colour from colourless to deep purple depending on radiation from its inclusions, adjacent radioactive material, evidence of REEs, or the presence of Y in particular (Deer et al., 1992 and Fayziyev, 1990). Fluorite is roughly pure, although traces of Y, Ce, and other rare-earth elements can replace the Ca (Berry et al., 2000). It has 88.33% Ca and 8.13% P according to ESEM (Fig. 11).
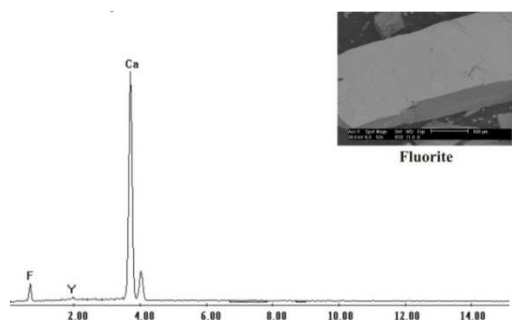
Fig. 11: ESEM image and EDX analysis data of fluorite, Wadi El Hora area, South Eastern Desert, Egypt.

3.d. Columbite (Fe,Mn)Nb$_2$O$_6$

Columbite is found as variable sized developed crystals with a black to brownish black color. It is confirmed by ESEM and contains 44.78% Nb, 18.42%Fe and 6.42% Mn (Fig. 12).
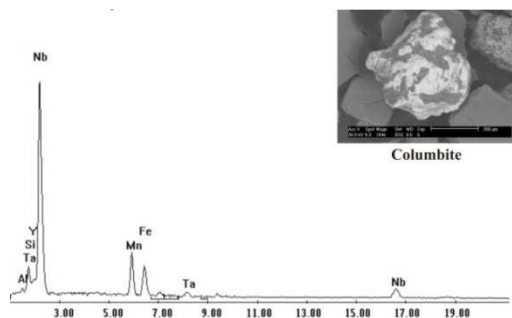
Fig. 12: ESEM image and EDX analysis data of columbite, Wadi El Hora area, South Eastern Desert, Egypt.

3.e. Molybdenite MoS$_2$

Molybdenite is found as flat needle plates. It is confirmed by ESEM and contains 69.84% Mo, and 27.88% S (Fig. 13).
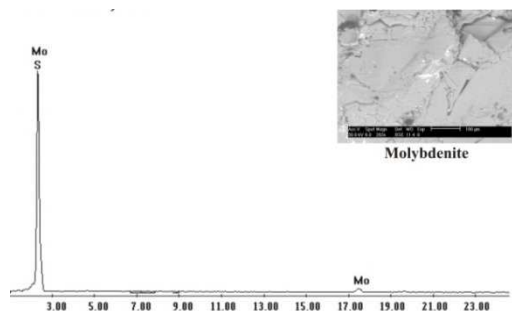
Fig. 13: ESEM image and EDX analysis data of molybdenite, Wadi El Hora area, South Eastern Desert, Egypt.

3.f. Zircon ZrSiO$_4$

Colors of zircon include reddish brown, yellow, and grey. Occasionally, Hf can replace Zr in amounts ranging from 1% to 4%, but if Hf predominates over Zr, the mineral is known as hafnon. Additionally, most zircons may be radioactive due to the presence of U or Th, which can occasionally replace Zr (Berry et al., 2000). ESEM has verified its composition, which is 67.22 % Zr, 17.47% Si, and 1.86% Hf (Fig. 14).
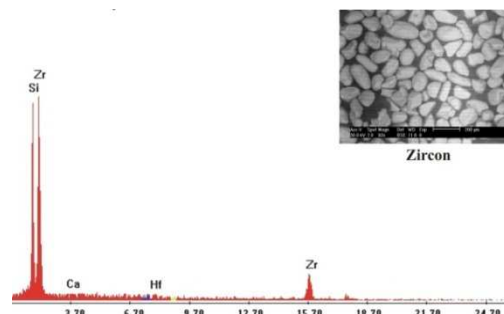
Fig. 14: ESEM image and EDX analysis data of zircon, Wadi El Hora area, South Eastern Desert, Egypt.

3.g. Pyrite FeS$_2$

Euhedral crystals with a cubic habit make up pyrite. When new, it has a light brassy yellow color that distinguishes it; but, when changed, it may take on hues ranging from deep crimson to black. It is verified by ESEM to have 32.75% Fe and 63.45% S (Fig. 15).
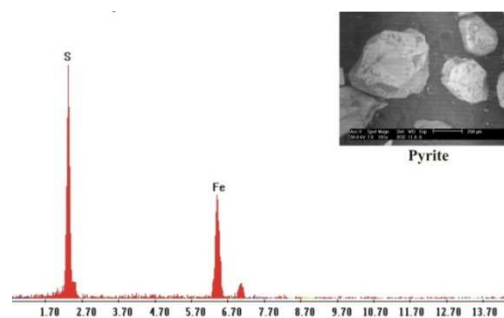
Fig. 15: ESEM image and EDX analysis data of pyrite, Wadi El Hora area, South Eastern Desert, Egypt.

3.h. Ilmenite FeTiO$_3$

Ilmenite is an iron-black colored. It is confirmed by ESEM and contains 37.12% Ti, and 28.45 Fe% (Fig. 16).
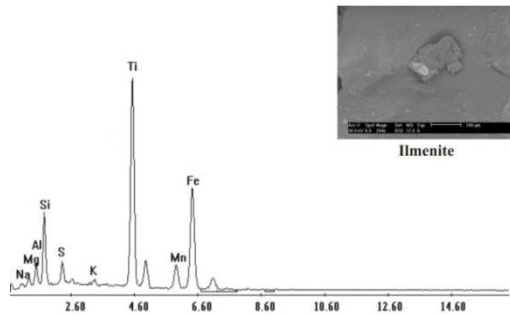
Fig. 16: ESEM image and EDX analysis data of ilmenite, Wadi El Hora area, South Eastern Desert, Egypt.

GEOCHEMISTRY

Sixteen representative samples of trachytes from Wadi El Hora area were selected for chemical analyses of major oxides, trace, and rare earth elements using XRF technique at the Nuclear Materials Authority (NMA), Egypt. The results together with CIPW normative mineral composition as well as some geochemical parameters listed in Tables 1, 2 and 3.

Classification, magma type and tectonic setting of the trachyte dykes in the studied area are denoted in these paragraphs according to some selected chemical variation diagrams.

The analysed samples are plotted in the trachyte field, which is supported by numerous diagrams, such as SiO_2-$Zr/TiO_2*0.0001$ (after Winchester and Floyd, 1977, Fig. 17), total alkalies-SiO_2 (after Le Maitre, 1989, Fig. 18), and total alkalies- SiO_2 (after Cox, et al., 1979), the discriminating boundary between alkaline and subalkaline/tholeiitic magma series after Miyashiro, 1978, Fig. 19), the studied trachyte samples plot in the alkaline field.
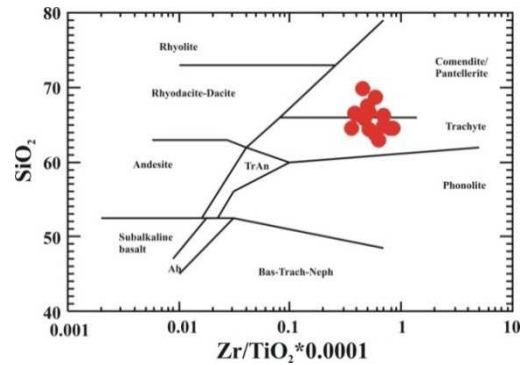
Fig. 17: SiO_2-$Zr/TiO_2*0.0001$ (Winchester and Floyd, 1977) classification diagram, Wadi El Hora area, South Eastern Desert, Egypt.
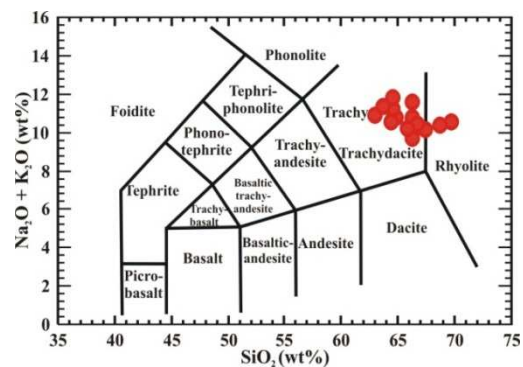
Fig. 18: Total Alkalies- SiO_2 (Le Maitre, 1989) classification diagram, Wadi El Hora area, South Eastern Desert, Egypt.
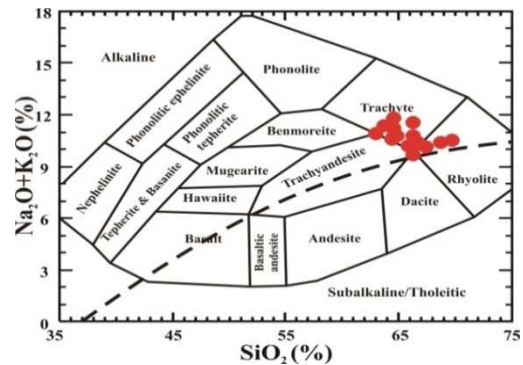
Fig. 19: Total Alkalies- SiO_2 (Cox, et al., 1979, the discriminating boundary between alkaline and subalkaline/tholeiitic magma series after Miyashiro, 1978), classification diagram, Wadi El Hora area, South Eastern Desert, Egypt.

Table 1: Major oxides and trace elements obtained from the chemical analysis of trachytes, Wadi El Hora area, south Eastern Desert, Egypt.

Sm. No.	1SH	2SH	3SH	4SH	5SH	6SH	7SH	8SH	9SH	10SH	11SH	12SH	13SH	14SH	15SH	16SH
	Major Oxides (%)															
SiO_2	64.82	64.33	66.24	64.47	66.69	62.98	63.66	64.49	65.75	66.29	66.59	69.75	67.46	64.54	66.32	68.72
Al_2O_3	14.87	16.81	15.29	15.66	14.76	16.33	15.45	16.37	16.12	16.1	17.89	15.36	17.11	17.57	16.56	15.27
TiO_2	0.18	0.26	0.23	0.17	0.27	0.18	0.23	0.18	0.29	0.19	0.29	0.31	0.25	0.32	0.34	0.19
Fe_2O_3	3.75	4.17	3.22	4.13	4.58	4.78	4.69	3.79	3.11	3.49	2.92	2.87	2.11	2.92	2.84	3.27
MnO	0.09	0.14	0.08	0.07	0.17	0.25	0.06	0.07	0.08	0.04	0.06	0.09	0.06	0.11	0.19	0.15
MgO	0.55	0.07	0.09	0.33	0.15	0.24	0.33	0.45	0.36	0.09	0.08	0.22	0.28	0.35	0.39	0.49
CaO	1.58	1.78	1.44	0.62	0.77	0.92	0.88	0.67	0.57	0.45	0.58	0.35	0.52	0.64	0.45	0.62
Na_2O	6.69	6.78	6.12	6.34	6.45	6.23	6.08	6.47	5.86	6.98	5.82	6.27	5.84	6.77	6.47	6.23
K_2O	4.11	3.78	3.56	4.89	3.96	4.68	5.27	5.36	4.34	4.59	4.43	4.27	4.32	4.02	4.32	4.17
P_2O_5	0.08	0.09	0.12	0.24	0.15	0.06	0.17	0.18	0.25	0.09	0.05	0.07	0.09	0.05	0.07	0.09
L.O.I	1.89	1.67	2.66	2.91	1.83	2.76	2.57	2.86	2.74	1.39	1.45	1.56	1.76	2.42	1.67	1.59
Total	98.61	99.88	99.05	99.83	99.78	99.41	99.39	100.89	99.47	99.7	100.16	101.12	99.8	99.71	99.62	100.79
	Trace elements (ppm)															
Cr	120	110	105	95	132	115	79	89	96	109	88	108	123	92	78	104
Ni	24	21	23	30	40	38	44	19	27	34	42	25	27	33	37	51
Cu	36	40	25	35	45	55	21	19	39	42	44	34	22	38	20	46
Zn	250	180	140	175	190	165	202	210	188	137	244	177	138	186	210	142
Zr	1228	1329	1158	1425	1382	1125	1357	1415	1346	1322	1120	1412	1237	1144	1322	1127
Rb	119	139	141	118	135	110	130	127	129	106	111	121	141	119	126	123
Y	80	79	65	90	77	89	93	85	92	64	88	61	91	71	68	81
Ba	62	65	78	58	44	88	60	59	169	199	67	79	56	155	146	59
Pb	19	22	35	26	20	18	12	10	42	39	28	68	61	30	26	28
Sr	44	36	27	38	30	35	29	31	28	48	42	38	31	34	27	30
Ga	31	30	28	31	32	30	29	27	33	32	34	25	36	26	24	33
V	10	9	4	3	6	5	7	9	10	10	9	8	9	7	4	5
Nb	268	239	240	248	269	280	277	301	219	249	266	241	245	267	274	222

Table 2: Norm obtained from the chemical analysis of trachytes, Wadi El Hora area, south Eastern Desert, Egypt.

Sm. No.	1SH	2SH	3SH	4SH	5SH	6SH	7SH	8SH	9SH	10SH	11SH	12SH	13SH	14SH	15SH	16SH
Q (S)	37.83	8.60	15.77	35.13	40.22	7.27	32.25	32.86	14.45	38.34	14.79	16.20	16.01	8.29	11.44	15.12
Or (KAS6)	25.13	22.77	21.85	29.84	23.91	28.64	32.20	32.34	26.54	27.62	26.55	25.37	26.06	24.44	26.36	24.86
Ab (NAS6)	0.00	58.35	53.66	0.00	0.00	54.48	0.00	0.00	51.20	0.00	49.83	53.23	50.34	58.81	56.40	53.08
An (CAS2)	0.00	4.31	3.84	0.00	0.00	2.83	0.00	0.00	1.41	0.00	2.62	1.13	2.09	2.96	0.64	1.36
C(A)	0.00	0.00	0.00	0.00	0.00	0.00	0.00	0.00	1.31	0.00	2.59	0.00	2.10	1.04	0.00	0.00
Ac(NFS4)	11.20	0.00	0.00	12.30	13.50	0.00	13.99	11.16	0.00	10.25	0.00	0.00	0.00	0.00	0.00	0.00
Ns(NS)	10.65	0.00	0.00	9.62	9.39	0.00	8.66	10.04	0.00	11.26	0.00	0.00	0.00	0.00	0.00	0.00
Di wo(CS)	1.80	0.21	0.27	0.72	0.73	0.64	1.09	0.97	0.00	0.33	0.00	0.09	0.00	0.00	0.52	0.50
Di en(MS)	1.42	0.18	0.23	0.55	0.38	0.55	0.85	0.77	0.00	0.23	0.00	0.07	0.00	0.00	0.45	0.43
Di fs(FS)	0.17	0.00	0.00	0.09	0.32	0.00	0.12	0.09	0.00	0.08	0.00	0.00	0.00	0.00	0.00	0.00
Hy en(MS)	0.00	0.00	0.00	0.30	0.00	0.07	0.00	0.38	0.93	0.00	0.20	0.48	0.71	0.90	0.56	0.80
Hy fs(FS)	0.00	0.00	0.00	0.05	0.00	0.00	0.00	0.04	0.00	0.00	0.00	0.00	0.00	0.00	0.00	0.00
Mt(FF)	0.00	0.47	0.27	0.00	0.00	0.31	0.00	0.00	0.27	0.00	0.20	0.30	0.20	0.37	0.64	0.49
He(F)	0.00	3.92	3.15	0.00	0.00	4.74	0.00	0.00	3.03	0.00	2.82	2.68	2.01	2.75	2.49	2.96
Il(FT)	0.00	0.00	0.00	0.00	0.00	0.35	0.00	0.00	0.00	0.00	0.00	0.00	0.00	0.00	0.00	0.00
Ap(CP)	0.18	0.20	0.27	0.54	0.33	0.14	0.38	0.40	0.56	0.20	0.11	0.15	0.20	0.11	0.16	0.20
Total	88.39	99.00	99.32	89.14	88.79	100.00	89.54	89.05	99.70	88.31	99.71	99.69	99.75	99.67	99.65	99.81

Table 3: REEs obtained from the chemical analysis of trachytes, Wadi El Hora area, south Eastern Desert, Egypt.

Sm. No.	1SH	3SH	5SH	7SH	9SH	11SH	13SH	15SH
REEs (ppm)								
La	140.00	125.00	175.00	150.00	135.00	220.00	160.00	145.00
Ce	320.00	299.00	375.00	285.00	298.00	399.00	365.00	310.00
Pr	33.00	29.00	37.00	33.00	36.00	50.00	40.00	28.00
Nd	139.00	105.00	112.00	120.00	119.00	99.00	120.00	95.00
Sm	19.00	18.00	17.00	29.00	30.00	26.00	24.00	25.00
Eu	4.12	3.23	2.14	3.65	3.77	3.26	2.99	2.05
Gd	18.95	14.15	13.59	15.37	15.82	17.75	14.62	16.22
Tb	2.99	2.35	2.62	3.21	3.07	2.78	2.54	2.71
Dy	17.11	14.29	14.29	16.31	18.26	16.59	14.81	18.12
Ho	2.49	2.82	3.82	2.89	2.92	3.49	2.85	3.31
Er	8.11	10.36	7.66	10.11	11.27	7.15	8.99	9.24
Tm	1.14	1.37	1.79	1.45	1.38	1.65	1.19	1.82
Yb	8.12	10.27	9.15	7.92	8.27	9.36	8.77	7.86
Lu	1.29	1.18	1.05	1.45	1.02	1.35	1.32	1.34
∑REE	715.32	636.02	772.11	679.36	683.78	857.38	767.08	665.67
∑LREE	651.00	576.00	716.00	617.00	618.00	794.00	709.00	603.00
∑HREE	64.32	60.02	56.11	62.36	65.78	63.38	58.08	62.67
∑LREE/∑ HREE	10.12	9.60	12.76	9.89	9.39	12.53	12.21	9.62
La / Yb	17.24	12.17	19.13	18.94	16.32	23.50	18.24	18.45
La / Sm	7.37	6.94	10.29	5.17	4.50	8.46	6.67	5.80
Gd / Lu	14.69	11.99	12.94	10.60	15.51	13.15	11.08	12.10
Gd / Yb	2.33	1.38	1.49	1.94	1.91	1.90	1.67	2.06
Eu/Eu*	0.02	0.02	0.03	0.02	0.02	0.04	0.03	0.03

The AFM ternary diagram (after Petro et al., 1979) indicates that the samples take the tensional trend (Fig. 20). According to the A/NK vs. A/CNK diagram of aluminum saturation (after Maniar and Piccoli, 1989) the samples show peralkaline to slightly peraluminous characters (Fig. 21). The total alkalis vs. SiO$_2$ diagram (Fig. 22) (after Irvine and Baragar, 1971); the shaded line area represents the continental oversaturated volcanics from the Cameroon (Fitton, 1987) indicate that the samples are of alkaline affinities.
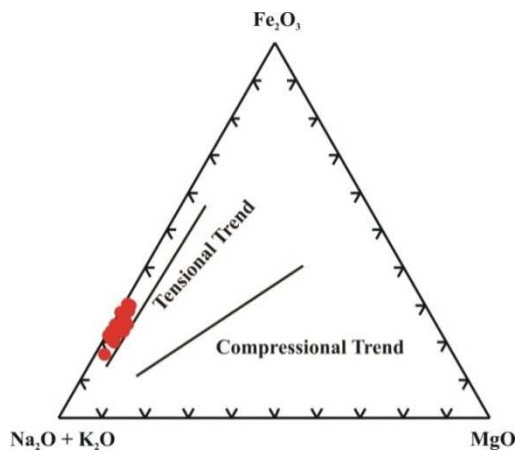
Fig. 20: Fe$_2$O$_3$-Na$_2$O+K$_2$O-MgO (after Petro et al., 1979), magma type diagrams, Wadi El Hora area, South Eastern Desert, Egypt.
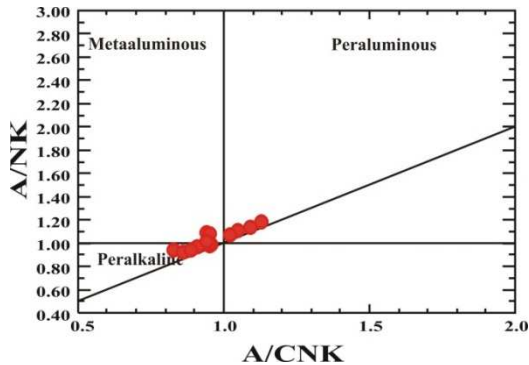
Fig. 21: A/NK vs. A/CNK (after Maniar and Piccoli, 1989), magma type diagrams, Wadi El Hora area, South Eastern Desert, Egypt.
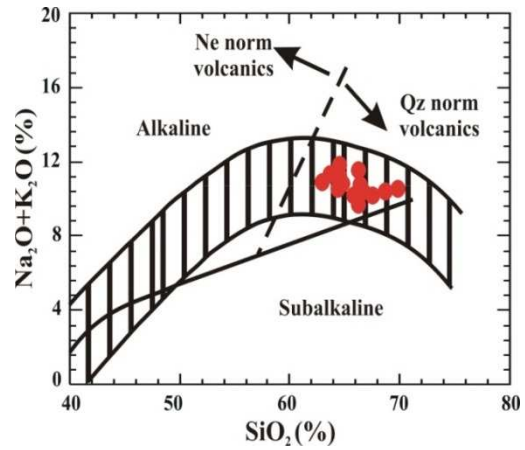
Fig. 22: Na$_2$O+K$_2$O vs. SiO$_2$ (after Irvine and Baragar, 1971; the line shaded area represents the continental oversaturated volcanics from the Cameroon (Fitton, 1987), magma type diagrams, Wadi El Hora area, South Eastern Desert, Egypt.

The binary relations of Nb vs. Y and Rb vs. (Nb + Y) of Pearce et al., 1984; indicate that the trachyte rocks of the studied area plot in the within plate field (Figs. 23 & 24).
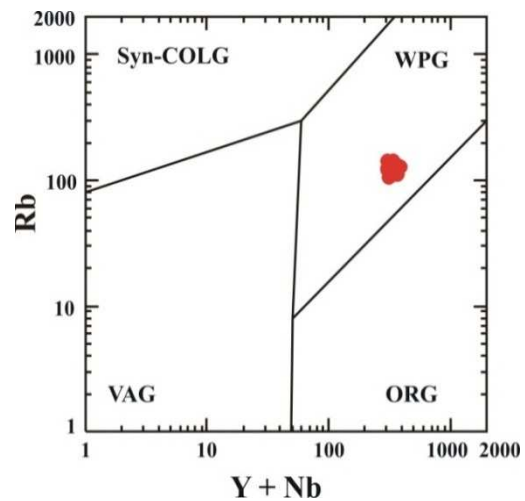
Fig. 23: Log Y+Nb-Log Rb, (after Pearce et al., 1984), tectonic setting diagrams, Wadi El Hora area, South Eastern Desert, Egypt.
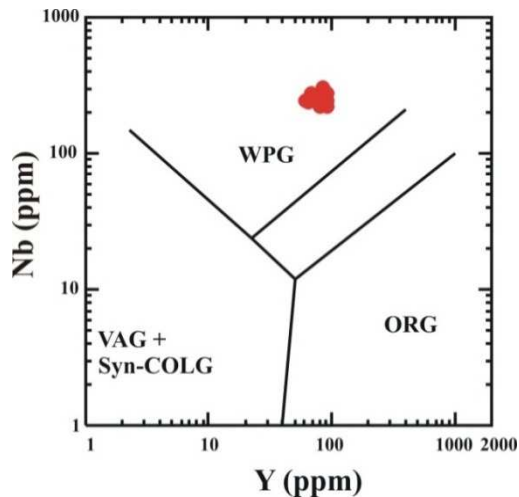
Fig. 24: Log Y-Log Nb, (after Pearce et al., 1984) tectonic setting diagrams, Wadi El Hora area, South Eastern Desert, Egypt.

On the chondrite-normalized diagram (Fig. 25), the trachyte rocks of Wadi El Hora area exactly show depletion in Eu and high enrichment of light REEs (660.5 ppm) according to the heavy REEs (61.59 ppm). Also, the chondrite-normalized trace elements diagram (Fig. 26) shows that, the trachyte rocks of W. El Hora area exhibit enrichments in Rb, Nb, light REEs and Zr and exhibit depletion in Ba and Sr due to consumption of these elements during the fractionation of plagioclase.
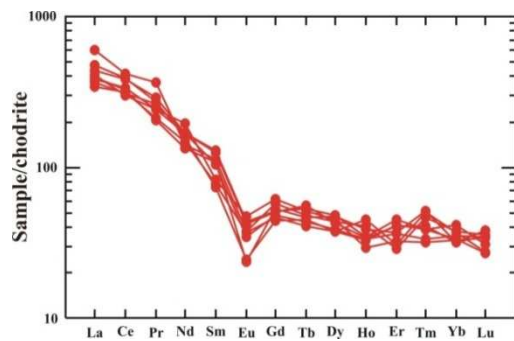
Fig. 25: Chondrite–normalized REEs patterns, (normalization values are after Sun and McDonough, 1989), Wadi El Hora area, South Eastern Desert, Egypt.
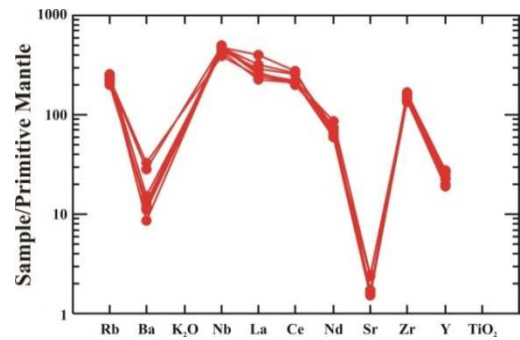
Fig. 26: Spider diagram of REEs and trace elements patterns, (normalization values are after Sun and McDonough, 1989), Wadi El Hora area, South Eastern Desert, Egypt.

SPECTROMETRIC PROSPECTING

The natural radioactivity of rocks stems mainly from their contents of U, Th and K^{40}. In the late magmatic stage, U and Th occur as U^{+4} and Th^{+4}. Th^{+4} is chemically stable, although oxygen fugacity regulates the stability and solubility of U^{+4} in silicate melts of different compositions. At lower oxygen fugacities, the stability of U^{+4} in silicate melts are higher (Finch and Ewing, 1992), and the uranium remains in the (+4) state like Th^{+4}, but when the oxygen fugacities increase U^{+5} and U^{+6} increase in magmatic silicate fluids and therefore the geochemical path of Th^{+4} and U^{+4} diverges. Rogers and Adams, (1969) stated that, in natural rocks the Th is three times as abundant as U, and the depletion or enrichment of uranium is illustrated according to this ratio. During differentiation of granitic rocks, generally; U and Th contents increase, although in some cases they decrease (Ragland et al., 1967) so the Th/U ratio can either increase or decrease as it is depending on the redox conditions, volatile contents, or alteration by endogens or supergene solutions (Falkum and Rose-Hansen, 1978). Rogers and Adams (1969) stated that the normal contents of U and Th in granitic rocks are 4 ppm and 11 ppm respectively. Uraniferous granites are defined according to Darnley (1982) as

any granitic masses containing U at least twice the Clarke value (4 ppm) whether or not they are associated with U mineralization. Uranium also tends to form the relatively soluble uranyl ion $(UO_2)^{+2}$ and mineralization may therefore arise through weathering and leaching of the host rock under oxidizing conditions with consequent removal of U and deposition elsewhere in fractures and faults (Gabelman, 1970). During fractionation, uranium may become enriched in the final fractions of magma, and the residual hydrothermal solutions may form U-rich veins (Goldschmidt, 1954).

The measurements are expressed in ppm for eU and eTh and % for K. In the field only gamma rays (which are of sufficient energy and have a long distance of penetration) could be detected. The instrument used in the ground γ-ray spectrometric survey measurements is RS-230. Ground γ-ray spectrometric survey can detect potassium (K%), equivalent uranium content (eU ppm), and equivalent thorium content (eTh ppm). Because U and Th are not gamma-ray emitters, the measurement of the gamma-rays released by their daughters is used to determine the eU and eTh using gamma-ray spectrometry. Uranium mobilisation (eU m) can be calculated as the difference between the measured eU and the expected original uranium, which is calculated by dividing the measured eTh by the average eTh/eU ratio in the crustal acidic rocks (original uranium = eTh/3.5 according to Clark et al., 1966), to give the leaching values of uranium (eU m = eU-eTh/3.5). Positive values indicate uranium addition by mobilization, whereas negative values indicate migration of uranium by leaching. If the surface U distribution is less than that of the hypothetical U distribution, the mobilization of U should has negative values, which mean that U is leaching out (Cambon, 1994).

The eU content in the trachyte dykes range from 0.6 to 197.1 ppm with an average 43.73 ppm, while the average of eTh is 109.35 ppm ranging from 2.4 to 626.30 ppm. The ratio of eU/eTh ranges from 0.25 to 0.31 with an average 0.40 and the eU mobilization is varying from -0.09 to 18.16 with an average of 12.49 as showing in (Table 4) and bar diagram (Fig. 27). The variation diagrams (Figs. 28:34) of the trachyte dykes show moderately positive for K% relation with each of eU (Fig. 28) and eTh (Fig. 29), strong moderately positive for eU relation with each of eTh (Fig. 30) and eU mobilization (Fig. 33), low weak positive relation between eU and the ratio eU/eTh (Fig. 31), weak positive for the relation of eTh with eU mobilization (Fig. 34) and finally low weak negative for the relation of eTh and the ratio eU/eTh (Fig. 32).
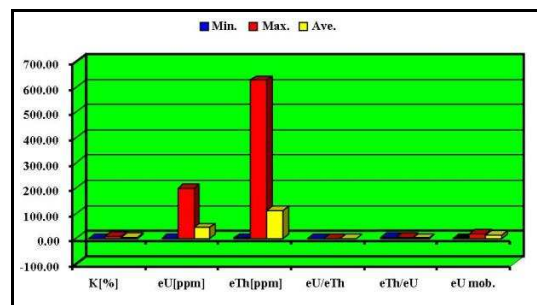
Fig. (27): Bar diagram showing the Min., Max., and aver. of K%, eU, eTh, eU/eTh, eTh/eU and eU mob. of radiometric reading in the trachyte rocks, Wadi El Hora area, South Eastern Desert, Egypt.

Table 4: Spectrometric analyses using RS-230 showing ranges and average contents of K (%), eU (ppm), eTh (ppm), eU/eTh and eU mobilization of trachytes, Wadi El Hora area, south Eastern Desert, Egypt.

Areas		(K %)		eU (ppm)		eTh (ppm)		eU/eTh		Mob.(eUm)= eU-(eTh/3.5)	
		Range	Av.	Range	Av.	Range	Av.	Range	Av.	Range	Av.
	N = 257	0.1 – 8.5	3.99	0.6 – 197.1	43.73	2.4 – 626.3	109.35	0.25 – 0.31	0.4	-0.09 – 18.16	12.49
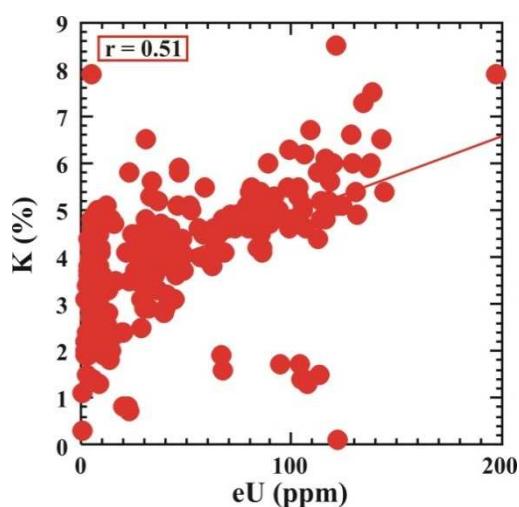
Fig. 28: K% vs. eU (ppm), Wadi El Hora area, South Eastern Desert, Egypt.
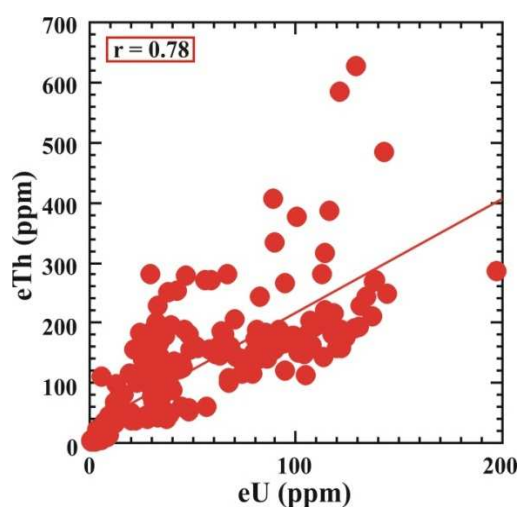
Fig. 30: eU (ppm) vs. eTh (ppm), Wadi El Hora area, South Eastern Desert, Egypt.
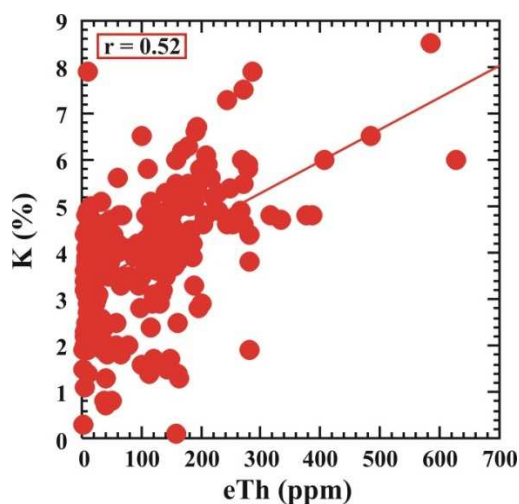
Fig. 29: K% vs. eTh (ppm), Wadi El Hora area, South Eastern Desert, Egypt.
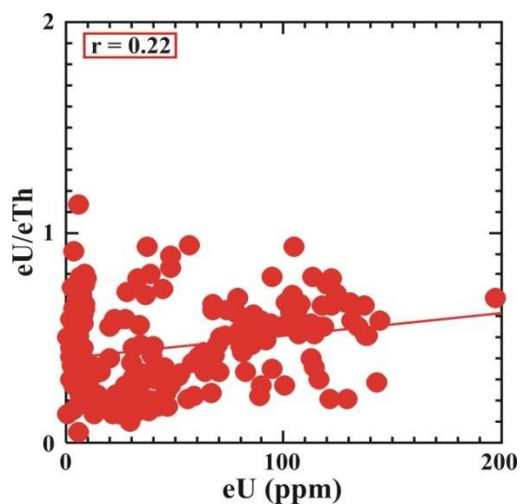
Fig. 31: eU (ppm) vs. eU/eTh ratio, Wadi El Hora area, South Eastern Desert, Egypt.
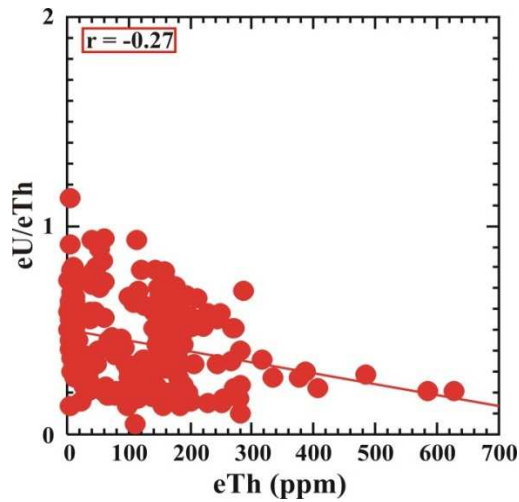
Fig. 32: eTh (ppm) vs. eU/eTh ratio, Wadi El Hora area, South Eastern Desert, Egypt.
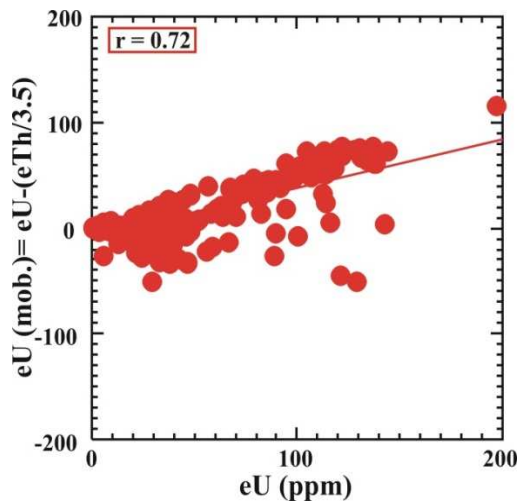
Fig. 33: eU (ppm) vs. eU mob., Wadi El Hora area, South Eastern Desert, Egypt.
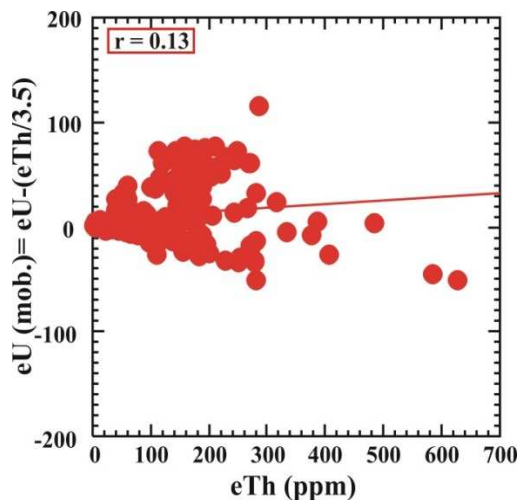
Fig. 34: eTh (ppm) vs. eU mob., Wadi El Hora area, South Eastern Desert, Egypt.

CONCLUSIONS

Wadi El Hora area Phanerozoic alkaline trachyte dykes are located at the southern Eastern Desert of Egypt. They are located between two strike-slip faults trending N-S and NW-SE. They consist essentially of feldspars (albite, oligoclase and sanidine), quartz, and alkali pyroxene (aegirine and aegirine-augite) with zircon, fluorite and opaques as accessory minerals whereas kaoline and sericite as secondary minerals. Wadi El Hora trachyte dykes could be considered as a good target for exploration of columbite and zircon. Detailed spectrometric analysis showed that the eU/eTh ratio fluctuates directly with eU concentrations and arbitrarily with eTh, showing that the radioelement concentration is controlled by post magmatic redistribution and also showing very wide ranges. The mineralogical study of the samples revealed the presence of kasolite, monazite, fluorite, columbite, molybdenite, zircon, pyrite and ilmenite minerals.

ACKNOWLEDGMENTS

REFERENCES

Abdalla, H.M.; Matsueda, H.; Saleh, G.M. and Ishihara, S., 2023. Phanerozoic Rare Earth Element Resources of Egypt: Metallogenetic and Mineral Exploration Constraints, The Phanerozoic Geology and Natural Resources of Egypt, https://doi.org/10.1007/978-3-030-95637-0.

Abdel-Rahman, A.M., 1995. Tectonic–magmatic stages of shield

evolution: the Pan-African belt in northeastern Egypt. Tectonophysics 242:223-240

Akaad, M.K., 1996. Rock succession of the basement on autobiography and assessment, Egypt. Geological Survey Mining Authority, 71:78P

Ali, S.; Abdallah, S.E; Abu Anbar, M.M.; Azzaz, S.A. and Alrashidi, K.N., 2022. Petrology of continental, OIB-like, basaltic volcanism in Saudi Arabia: Constraints on Cenozoic anorogenic mafic magmatism in the Arabian Shield. Front. Earth Sci. 10: 921-994. doi:10.3389/feart.2022.921994.

Aly, M.M. and Moustafa, M.M., 1984. Major chemistry statistics characterizing common igneous rocks of Egypt. 9th Inter. Cong. Stat. Comp. Sci. Res., Ain Shams Univ., Cairo

Amer, T.E.; Saleh, G.M. and El-Hazek, M.N., 2002. Geological and flotation beneficiation characteristics of the newly discovered refractory complex ore of Gabal El-Homur, South Eastern Desert, Egypt. Journal of Environmental Research, 4:206-222

Baliey, D.K., 1980. Volatile flux, geotherms and the generation of the kimberlite –carbonatite – alkaline magma spectrum. Mineralogical Magazine, 43:695-699

Berry, L.G.M.; Mason, B. and Dietrich, R.V., 2000. Mineralogy. CBS Publishers and Distributors, New Delhi, India. 561pp.

Cambon, A.R., 1994. Uranium deposits in granitic rocks. Notes on the national training course on uranium geology and exploration. Organized by IAEA and NMA, Jan. 1994, Cairo, p. 8-20

Clark, S.P.Jr.; Petrman, Z.E. and Heier, K.S., 1966. Abundance of

uranium, thorium and potassium, In: S.P. Clark, Jr., Editor), Handbook of Physical constraints, Geol. Soc. Am. Mem. 97, Section 24:521-541

Cox, K.G.; Bell, J.D. and PanKhurst, R.J., 1979. The interpretation of igneous rocks. London, Allen and Unwin, 450pp

Darnley, A.G., 1982. "Hot granites" some general remarks. In: Maurice, Y. J. (ed.), Uranium in granites. Geol. Surv. Canada, Paper No. 81, 23:1-10

Davidson, J.P. and Wilson, I.R., 1989. Evolution of an alkali basalt-trachyte suite from G.Marra volcano, Sudan, Through assimilation and fractional crystallization. Earth Planetary Science Letters, 95:141-160

Deer, W.A.; Howie, R.A. and Zussman, J., 1992. An introduction to the rock formingminerals. Longman group limited, England. Second edition. 696pp.

El Amin, H. and Bassiony, M.W., 1987. Geologicaland petrological contribution to invistigations at Gebel Silaia area, Eastern Desert, Egypt, Egypt. Jour. Geol., 31

El Ramly, M.F.; Budanov, V.I. and Hussein, A.A., 1971. The alkaline rocks of Southeastern Desert, Egypt. Egypt Geol. Surv. Paper, 53. Cairo, Egypt, 170pp.

El Tohamy, A.M., 2011. Mineralogy and Geochemistry of the Volcanic Rocks of Gabal El Ghorfa, South Eastern Desert, Egypt. M. Sc. Thesis. Faculty of Science, Benha Univ., Benha: 165.

El-Manharawy, M.S., 1972. Isotopic ages and origin of some uranium bearing volcanic rocks in Egypt. M. Sc. Thesis, Cairo Univ

El-Shazly, E.M., 1977. The geology of the Egyptian region. In: The ocean basins and margins, (Edited by Nairn A.E., Kanes, W. H., and

stehli, F.G.), 4A:379-444, New York

Falkum, T. and Rose-Hansen, J., 1978. The application of the radioelement studies in solving petrological problems of the Precambrian intrusive Homme granite in the Flekkefjord area, South Norway. Chem. Geol., 239:73-86

Fayziyev, A.R., 1990. Yttrium in fluorite from endogenous shows in USSR. Translated from Geokhimiya, 7:1037-1042

Finch, J.R. and Ewing, C.R., 1992. The corrosion of uraninite under oxidizing conditions. Journal Nuclear Materials 190:133-156

Fitton, J.G., 1987. The Cameroon line, West Africa: A comparison between oceanic and continental alkaline volcanism. In Alkaline Igneous Rocks. Royal Society Special Publication, 30:273-291

Gabelman, J.W., 1970. Speculations on the uranium ore fluid. In: Uranium Exploration Geology, 315-330

Ghazaly, M., 1996. A contribution to the geology and geochemistry of the granites of SILAIAAND El Homur south Eastern Desert, Egypt. Mineralogist, 8:41-57

Goldschmidt, V.M., 1954. Geochemistry. Oxford: University Press, Oxford. 730pp.

Gourgaud, A. and Maury, R.C., 1984. Magma mixing in alkaline series: an example from Sancy volcno (Mont Dore, Massif, Central, Frace). Bulletin Volcanology, 47:827-847

Hamdy, M. M.; Waheeb, A.G.; Aly, S. M.; Farag, N. M. and Sadek, A. F., 2017. Phanerozoic extensional faulting and alteration control on uranium mineralization in trachytes of the Central Eastern Desert of Egypt. Journal of African Earth Sciences 136, 282-304.

Harris, N.B.W., 1982. The petrogenesis of alkaline intrusives from Arabia and northeast Africa and their implications for withinplate magmatism. Tectonophysics 83:243–258

Hashad, A.H. and El-Reedy, M.W., 1979. Geochronology of anorogenic alkalic rocks, southeastern Desert, Egypt. Ann. Geol. Surv. Egypt, 9:81–101

Hashad, A.H. and Mahfouz, S., 1976. On the geochemistry of W. Kareim volcanics, Egypt. Chemi. Erde (Geochemistry), 35:317-326

Hashad, A.H.; Hassan, M.A. and Aboul Gadayel, A.A., 1978. Trace element variations in the alkaline volcanics of W. Natash, Egypt. Bulletin faculty Earth Science King Abdulaziz University., Jeddah, 2 A, 195-204.

Hashad, A.H.; Sayyah, T.R. and El-Manharawy, M.S., 1981. Isotopic composition of strontium and origin of W. Kareim, Eastern Desert, Egypt. Journal Geology, 25(1-2):141-147

Heikal, M.T., 2003. Model for the origin of the Um Shaghir-Um Khors alkaline trachyte plugs, Central Eastern Desert, Egypt. The Third International Conference on the Geology of Africa, 1:233-253.

Hunting Geology and Geophysics (1967. Assessment of the mineral potential of the Aswan region, UAR Internal Report, Geol. Surv. Egypt, 138 p

Ibrahim, M.E.; Attawiya, M.Y.; Osman, A.M. and Ibrahim, I.H., 2002. Occurrence of uranium bearing minerals in Um Safi pyroclastics, Central Eastern Desert, Egypt. Egyptian. Journal of Geology, 46-1:39-54

Irvine, T.N. and Baragar, W.R.A., 1971. A guide to the chemical classification of the common volcanic rocks. Canadian Journal

of Earth Sciences, V. 8. p. 523-548.

Kamel, A.F.; Mansour, S.I. and Ibrahim, M.E., 1985. The study of the radioactive dyke at Um Domi area, Southeastern Desert, Egypt. (Internal Report). 14p

Kröner, A., 1985. Ophiolites and the evolution of tectonic boundaries in the Late Proterozoic Arabian–Nubian Shield of northeast Africa and Arabia. Precam Res 27:277–300

Le Maitre, R.W., 1989. A classification of igneous rocks and glossary of terms: Recommendations of the International Union of Geological Sciences, Subcommission on the Systematics of Igneous Rocks. Blackwell, Oxford. 193pp

Leroy, J.L. and Aniel, B.G., 1991. Uranium behavior in volcanic environments: source-rocks and concentration mechanisms. Transport and Deposition of Metals, Balkema, Rotterdam, 321-324

Maniar, P.D. and Piccoli, P.M., 1989. Tectonic discrimination of granitoids. Geological Society of America Bulletin, 101: 635-643

Meneisy, M.Y., 1990. Volcanicity. In: Said R (ed) The geology of Egypt. Balkema, Rotterdam, 157-172

Miyashiro, A., 1978. Nature of alkalic volcanic rock series. Contribution to Mineralogy and Petrology 66:91-104.

Pearce, J.A.A.; Harris, N.B.W. and Tindle, A.G., 1984): Trace element discrimination diagrams for the tectonic interpretation of granitic rocks. Journal of Petrology, 25: 956-983

Petro. W.L. Vogel, T.A. and Wilband, J.T., 1979. Major element chemistry of plutonic rock suites from compressional and extensional plate boundaries. Chem. Geol., 26:217-235

Price, R.C.; Johnson, R.W.; Gray, C.M. and Frey, F.A., 1985. Geochemistry of phonolites and Trachyte from the summit region of Mt. Kenya. Contributions Mineralogy Petrology, 89:394-409

Ragland, P.C.; Billing, G.K. and Adams, J.A., 1967. Chemical fractionation and its relationship to the distribution of thorium and uranium in a zoned granitic batholiths. Geochem. Csmochem. Acta, 31:17-37

Ressetar, R.; Nairn, A.E.M. and Monrad, J.R., 1981. Two phases of cretaceous – Tertiary magmatism in the Eastern Desert of Egypt: Paleomagnetic, chemical and K-Ar evidence. Tectonophysics, 73:169-193

Rogers, J.J.W. and Adams, J.A.S., 1969. Uranium and thorium, In: K. H. Wedepohl (ed.), Handbook of geochemistry. Berlin, Springier-Verlag, v. 113, 92-B-1 to 92-0-8 and 90-Bb-1 to 90-00-5, 201pp.

Saleh, G. M.; Kamar, M. S. and Mira H. I., 2021. Phanerozoic Minor Volcanics and Intrusives of the Arabian-Nubian Shield, The Geology of the Arabian-Nubian Shield, Regional Geology Reviews, https://doi.org/10.1007/978-3-030-72995-0_26.

Saleh, G.M., 2012. Geochemical characteristic of some mineralization in Wadi El Gemal_ Abu Ghusun area South Eastern Desert, Egypt. Report, 45pp.

Saleh, G.M.; Emad, B.M.; Abdel Kader, I.B. and Sakr, R.M., 2021. The possible source of uranium mineralization in felsic volcanic rocks, Eastern Desert, Egypt of the Arabian-Nubian Shield: Constraints from whole-rock geochemistry and spectrometricun prospection, Acta Geochim., https://doi.org/10.1007/s11631-021-00472-4

Saleh, G.M.; Ibrahim, I.H.; Azab, M.S.; Abd El Wahed, A.A.; Ragab, A.A. and Ibrahim, M.E., 2004. Geologic and Spectrometric Studies on Um Domi Phanerozoic Trachyte Plug, South Eastern Desert, Egypt. The Sixth International Conference On Geochemistry: 329-345.

Saleh, G.M.; Kamar, M.S.; Rashed, M.A. and El-Sherif, A.M., 2015. Uranium Mineralization and Spectrometric Prospecting along trenches of Um Safi area, Central Eastern Desert of Egypt. Geoinfor Geostst.: An overview: 3:1.

Saleh, G.M.; Oraby, F.; Abu El Hassan, E.; Azab, M.S.; Mansour, G.M.; Rashed, M.A. and El Sherief, A., 2007. Um Khors alkaline volcanics, Central Eastern Desert, Egypt: Geochemical constraints, spectrometric prospecting and mineralization. 10th International Mining, Petroleum and Metallurgical Engineering Conference, March 6-8:185-204.

Soliman, M.M., 1975. Geology, geochemistry and mineralization of some younger granite masses in the Eastem Desert of Egypt Ph. D. Thesis, Mansoura, Univ.

Stairs, M.; Morteani, G.; Fuganti, A. and Drach, V., 1991. K-Ar ages, Srisotopic composition and chemistry of late Cretaceous-Tertiary basalts from the Nubian Desert (northern Sudan). European Journal Mineralogy, 3:943-955

Stoeser, D.B., 1986. Distribution and tectonic setting of plutonic rocks of the Arabian Shield. Journal of African Earth Sciences, 4:21-46

Sun, S.S. and McDonough, W.F., 1989. Chemical and isotopic systematics of oceanic basalts: implications for mantle composition and processes. In: Saunders AD, Norry (eds) Magmatism in the ocean basins, The Geological Society, London, 42:313-345

Winchester, J.A. and Floyd, P.A., 1977. Geochemical discrimination of different magma series and their differentiation products using immobile elements. Chemical Geology 20:325-343

دراسات جيولوجية وجيوكيميائية وطيفية على جدد التراكيت بمنطقة وادي الحرة جنوب الصحراء الشرقية، مصر

إبراهيم بديع عبدالقادر

تقع جدد وادي الحرة القلوية في جنوب الصحراء الشرقية لمصر؛ بين فالقين مضربيين في اتجاه N-S و NW-SE بين خطي عرض ٢٣° ٥١` ٤٨`` و٢٤° ٠٠` ٥١`` شمالا وخطي طول ٣٤° ٥٠` ١١`` و٣٤° ٥٨` ٤٦`` شرقا على بعد حوالي ٨ كم جنوب شرق منجم درهيب للتلك وحوالي ٤٠ كم جنوب غرب الشيخ الشاذلي. تتكون جدد التراكيت القلوية أساسًا من الفلسبار (ألبايت، أوليجوكليز، وسانيدين)، والكوارتز، والبيروكسين القلوي (إيجيرين وإجيرين–أوجيت) مع الزركون والفلوريت والمعادن المعتمة كمعادن إضافية، وأخيراً الكاولين والسريسيت كمعادن ثانوية.

جدد التراكيت غنية بعناصر عالية شدة المجال Nb و Zr و Y، كما أنها تعرض أيضًا صهارة قلوية توسعية تكتونية نشأت في بيئة بين لوحية. تظهر أنماط العناصر الأرضية النادرة (REE) شذوذًا سلبيًا في Eu وهي موحدة إلى حد كبير ومجزأة بشكل كبير. يمكن اعتبار جدد التراكيت هذه هدفًا جيدًا لاستكشاف الكولومبيت والزركون. وفقًا لتحليل قياس الطيف الإشعاعي، يتم التحكم في تركيزات العناصر المشعة عن طريق إعادة توزيع المواد المنصهرة

يظهر ذلك في تغيرت نسبة eU/eTh المباشرةً مع تركيزات eU وبطريقة مبعثرة مع eTh. تُظهر القياسات الإشعاعية لجدد التراكيت في منطقة الدراسة تباينًا كبيرًا جدًا في محتويات eU حيث يتراوح محتوى eU من ٠.٦ إلى ١٩٧.١ جزء في المليون بمتوسط ٤٣.٧٣ جزء في المليون ويتراوح محتوى eTh من ٢.٤ إلى ٦٢٦.٣ جزء في المليون بمتوسط ١٠٩.٣٥ جزء في المليون. تؤكد الدراسة المعدنية وجود معادن الكازوليت والمونازيت والفلوريت والكولومبيت والموليبدينيت والزركون والبيريت والإلمنيت.